International Conference on Modeling and Simulation of Microsystems MSM 2002, April 22-25 2002, San Juan, Puerto Rico, USA; www.cr.org
© Computational Publication

Large Scale FDTD Simulation for Microoptics and Metamaterial Investigations - Current Possibilities and Verification Benchmarks

Andreas Hieke * and Robert Tramel **

CFD Research Corporation, *Sunnyvale, CA 94087, USA, email ahi@ieee.org ; **Huntsville, AL 35805

ABSTRACT

The study of microsystems containing photonic crystals (PC) and meta-materials are rapidly growing fields of research. Finite-Difference Time-Domain (FDTD) full wave electromagnetic solvers are now increasingly used to investigate and design such systems. However, in order to simulate the electromagnetic response of such complex systems containing a large number of dielectric and/or conducting scatterers (e.g. band-gap effects) it is of foremost importance to gain sufficient evidence that the code being used is operating correctly.

PEC and dielectric cylinders provide an important initial object to study the accuracy of scattering solutions. Time-depended analytical wave solution for complete 2D spaces, including inside materials, have been mapped and compared to FDTD solutions of the named examples using shape-conformal meshes. Therewith the basis has been established to execute reliable, large scale FDTD simulation containing several million cells.

Keywords: FDTD, Maxwell's equations, scattering, photonic crystal, unstructured mesh, integrated optics

1 INTRODUCTION

Integrated optical circuits and certain advanced microwave components containing photonic crystals and meta-materials are increasingly developed and incorporated into products [1]-[6]. The behavior of such materials and systems is typically very complicated, even counter intuitive, while the application of analytical methods is limited or yields little insight into the creation of observed effects.

For example, although the notion of a forbidden energy band (bang gap) is well-understood and common from solid state theory, its origin as a collective phenomena of a large number of electromagnetic scatterers is less obvious. There are different notions as to how a PC is established, specifically which conditions need to be satisfied in order tailor a photonic crystal for a certain band gap. Factors that mainly impact the property of repetitive dielectric structures are the relative permittivity of the single scatterers, their mutual distance and shape. There are also intriguing similarities with X-ray diffraction (XRD) theory, specifically XRD investigations on colloidal systems [9].

In many practical instances, PCs of finite size (limited number of unit cells), including imperfections in periodicity and shape are considered and the behavior of the system in the time domain is of particular interest. In these cases the application of full wave Maxwell solvers is essential [12].

2 VALIDATION CASES

Beside obvious cases of instability, FDTD simulations can yield reasonably appearing results that are inaccurate. A user has to develop a 'feel' for acceptable mesh configurations and aspect ratio changes since such rules are not yet incorporated in intelligent agents that would control the meshing process. Eventually, simulation results must be trusted sufficiently that they can form the basis for devices to be fabricated.

2D PCs are, in the majority of cases, built from arrays of dielectric cylinders. Ultimately, the systems to be modeled contain a large number of such scatterers. It is, therefore, of value to find the correlation between mesh density and achievable accuracy. EM wave scattering on dielectric and perfectly electrically conducting (PEC) cylinders are two of the few known cases for which analytical solution satisfying Maxwell's equations can be found. For the first time, using the computer algebra system MathCAD, time-depended analytical wave solution for complete 2D spaces, including inside materials, have been mapped and compared to FDTD solutions. This allowed a new level of verification and insight, since usually only static 1D total cross-sections are compared.

2.1 Scattering on an infinite PEC cylinder

The solution for the *z*-component of the scattered magnetic field from a PEC cylinder with a radius *R* subjected to a monochromatic plane TE_z polarized wave with a wavelength of λ is given in (1) [10]. J_n denotes first kind Bessel functions of *n*-th order and $H_n^{(2)}$ second kind Hankel function of *n*-th order. It is obviously necessary to restrict *n* in (1) and (3)-(5) to a finite number. Tests confirmed that a range of n=[-8,8] is sufficient to achieve a relative accuracy better then $|\Delta B/B|<10^{-3}$ for the scattered field solution and n=[-16,16] for the total field solution.

Fig. 1 illustrates the solutions from the FDTD solver CFD-MAXWELL and from MathCAD. Typical derivations on the order of 2% have been achieved using a shape-conformal mesh with only 3000 cells.

$$ {}_{s}B_z(r,\varphi,t) = B_0 e^{-i\omega t} \sum_{n=-\infty}^{n=+\infty} \frac{\dfrac{\partial}{\partial\left(\dfrac{2\pi R}{\lambda}\right)} \mathrm{J_n}\left(\dfrac{2\pi R}{\lambda}\right)}{\dfrac{\partial}{\partial\left(\dfrac{2\pi R}{\lambda}\right)} \mathrm{H_n^{(2)}}\left(\dfrac{2\pi R}{\lambda}\right)} \left[i^{-n}\, \mathrm{H_n^{(2)}}\left(\dfrac{2\pi r}{\lambda}\right) e^{in\varphi} \right] \tag{1} $$

$$ {}_{s}E_z(r,\varphi,t) = \begin{vmatrix} {}_{sv}E_z(r,\varphi,t) & \forall\, r > R \\ {}_{sm}E_z(r,\varphi,t) \;-\; {}_{i}E_z(r,\varphi,t) & \forall\, r \le R \end{vmatrix} \tag{2} $$

$$ {}_{i}E_z(r,\varphi,t) = E_0 e^{-i\omega t} \sum_{n=-\infty}^{n=+\infty} \left[i^{-n}\, \mathrm{J_n}\left(\frac{2\pi r}{\lambda}\right) e^{in\varphi} \right] \tag{3} $$

$$ {}_{sv}E_z(r,\varphi,t) = E_0 e^{-i\omega t} \sum_{n=-\infty}^{n=+\infty} \frac{\left[\dfrac{\partial}{\partial\left(\dfrac{2\pi R}{\lambda}\right)} \mathrm{J_n}\left(\dfrac{2\pi R}{\lambda}\right)\right] \cdot \mathrm{J_n}\left(\dfrac{2\pi R\sqrt{\varepsilon_r}}{\lambda}\right) \;-\; \sqrt{\varepsilon_r}\, \mathrm{J_n}\left(\dfrac{2\pi R}{\lambda}\right) \cdot \left[\dfrac{\partial}{\partial\left(\dfrac{2\pi R\sqrt{\varepsilon_r}}{\lambda}\right)} \mathrm{J_n}\left(\dfrac{2\pi R\sqrt{\varepsilon_r}}{\lambda}\right)\right]}{\sqrt{\varepsilon_r} \cdot \left[\dfrac{\partial}{\partial\left(\dfrac{2\pi R\sqrt{\varepsilon_r}}{\lambda}\right)} \mathrm{J_n}\left(\dfrac{2\pi R\sqrt{\varepsilon_r}}{\lambda}\right)\right] \cdot \mathrm{H_n^{(2)}}\left(\dfrac{2\pi R}{\lambda}\right) \;-\; \mathrm{J_n}\left(\dfrac{2\pi R\sqrt{\varepsilon_r}}{\lambda}\right) \cdot \left[\dfrac{\partial}{\partial\left(\dfrac{2\pi R}{\lambda}\right)} \mathrm{H_n^{(2)}}\left(\dfrac{2\pi R}{\lambda}\right)\right]} \left[i^{-n}\, \mathrm{H_n^{(2)}}\left(\frac{2\pi r}{\lambda}\right) e^{in\varphi} \right] \tag{4} $$

$$ {}_{sm}E_z(r,\varphi,t) = E_0 e^{-i\omega t} \sum_{n=-\infty}^{n=+\infty} \frac{\left[\dfrac{\partial}{\partial\left(\dfrac{2\pi R}{\lambda}\right)} \mathrm{H_n^{(2)}}\left(\dfrac{2\pi R}{\lambda}\right)\right] \cdot \mathrm{J_n}\left(\dfrac{2\pi R}{\lambda}\right) \;-\; \mathrm{H_n^{(2)}}\left(\dfrac{2\pi R}{\lambda}\right) \cdot \left[\dfrac{\partial}{\partial\left(\dfrac{2\pi R}{\lambda}\right)} \mathrm{J_n}\left(\dfrac{2\pi R}{\lambda}\right)\right]}{\left[\dfrac{\partial}{\partial\left(\dfrac{2\pi R}{\lambda}\right)} \mathrm{H_n^{(2)}}\left(\dfrac{2\pi R}{\lambda}\right)\right] \cdot \mathrm{J_n}\left(\dfrac{2\pi R\sqrt{\varepsilon_r}}{\lambda}\right) \;-\; \sqrt{\varepsilon_r}\, \mathrm{H_n^{(2)}}\left(\dfrac{2\pi R}{\lambda}\right) \cdot \left[\dfrac{\partial}{\partial\left(\dfrac{2\pi R\sqrt{\varepsilon_r}}{\lambda}\right)} \mathrm{J_n}\left(\dfrac{2\pi R\sqrt{\varepsilon_r}}{\lambda}\right)\right]} \left[i^{-n}\, \mathrm{J_n}\left(\frac{2\pi r\sqrt{\varepsilon_r}}{\lambda}\right) e^{in\varphi} \right] \tag{5} $$

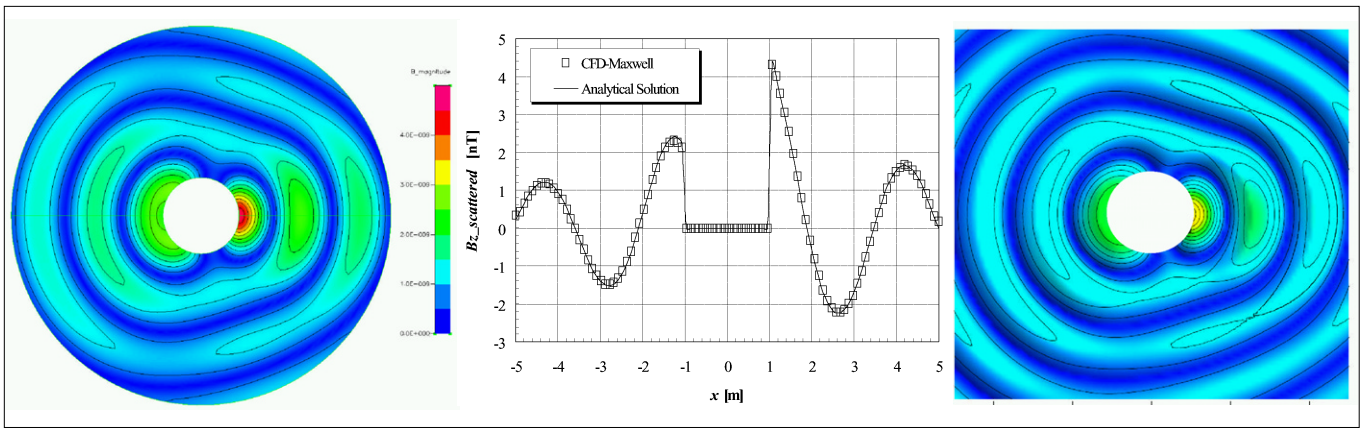

Fig 1: Scattering of a plane electromagnetic wave on an infinite PEC cylinder with diameter d=2R (normal incident, TE_z polarization, +x-propagation); λ/d=1.5; (solver in scattered field mode, scattered field plotted) **left:** FDTD simulation (ca. 3000 cells), contour plot of $|{}_{s}B_z\ (r,\ \varphi,\ 2\pi\ \tau/T)|$ at constant, random phase angle τ after steady state is reached; **middle:** comparison of analytical and FDTD solution for ${}_{s}B_z\ (x)|_{y=0}$ at same phase angle; **right**: 2D mapping of the analytical solution for $|{}_{s}B_z\ (r,\ \varphi,\ 2\pi\ \tau/T)|$ obtained in MathCAD

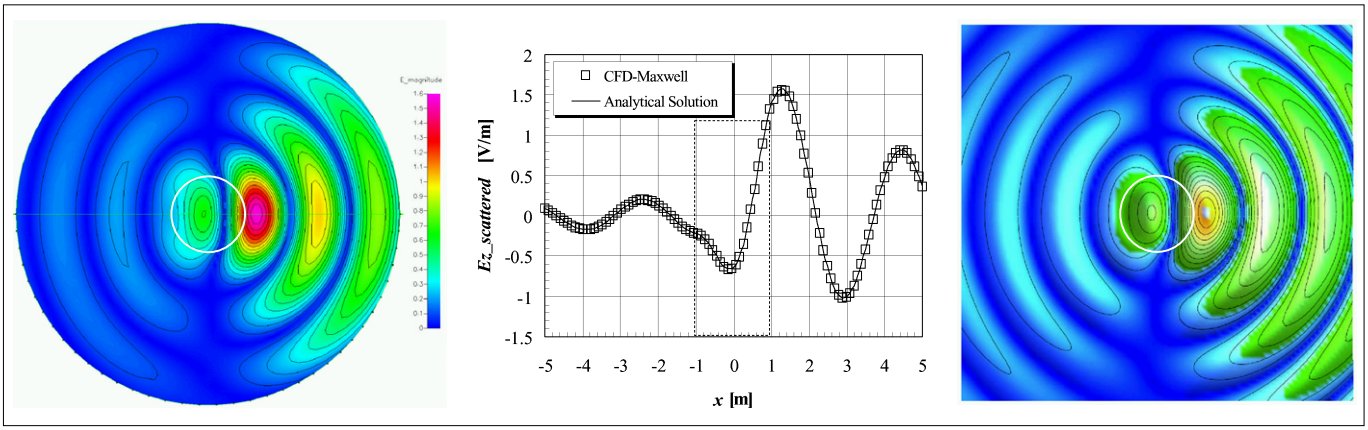

Fig 2: Scattering of a plane electromagnetic wave on an infinite dielectric cylinder with ε_r=2, diameter d=2R (normal incident, TM_z polarization, +x-propagation); λ/d=1.5; (solver in scattered field mode, scattered field plotted) **left**: FDTD simulation (ca. 4000 cells), contour plot of $|{}_sE_z\,(r, \varphi, 2\pi\,\tau/T)|$ at constant, random phase angle τ after steady state is reached (cylinder wall indicated by white circle); **middle:** comparison of analytical and FDTD solution for ${}_sE_z\,(x)|_{y=0}$ at same phase angle; **right**: 2D mapping of the analytical solution for $|{}_sE_z\,(r, \varphi, 2\pi\,\tau/T)|$ obtained in MathCAD

2.2 Scattering on a dielectric cylinder

The solution for the z-component of the scattered electric field from an infinite dielectric cylinder with a radius R subjected to a monochromatic plane TM_z polarized wave with a wavelength of λ is given in (2)-(5) [10]. The analytical solution for the scatted field has to be composed (2) from different equations for the incident field ${}_iE_z\,(r,\varphi,t)$ (3), the field outside the cylinder ${}_{sv}E_z\,(r,\varphi,t)$ (4), and the field inside the cylinder ${}_{sm}E_z\,(r,\varphi,t)$ (5). The same range for n is used as in the previous example.

Fig. 2 shows the results from the FDTD solver and from MathCAD. Again, typical derivations on the order of 2% have been achieved with only 4000 cells. The inherent capability of CFD-Maxwell to operate on mixed structured/unstructured meshes [13] has been essential. Additional test cases involving different wavelength-to-scatterer size ratios and permittivities have confirmed these accuracies.

2.3 Advanced examples and practical aspects

As a second step, larger cases such as the scattering behavior of 'mini crystals' (Fig. 2) have been investigated as well as true 3D scattering configurations with over 10^6 cells (Fig 4). Due to the time-dependent phenomena simulated, very large amounts of data on the order of 10 to 20Gbyte can be generated. Typically, MPEG-2 movies are created from these data to allow visualization of the evolution of the solutions, the educational effect of which has been found to be invaluable. To reduce the penalty of disk operations on the overall execution time, the system used (2 PIII 1GHz, 2GByte, NT4.0) employed a quadruple RAID0 disk array with a sustained I/O speed of 50 to 80MByte/s and negligible CPU utilization. Large main memory size and motherboards with fast memory access (bus width, access mode, high-end chip set) are advisable.

3 SUMMARY

Detailed analytical verifications have confirmed the high accuracy CFD-Maxwell operating on unstructured meshes provides for EM scattering problems. Very large cases with up 10 million unstructured cells are now possible on desktop workstations. Memory access and operating system (OS) limitations may soon need consideration for i386 CPUs. Systems with physical address extension (PAE) mode surpassing the 32bit /4GByte limit are recommended.

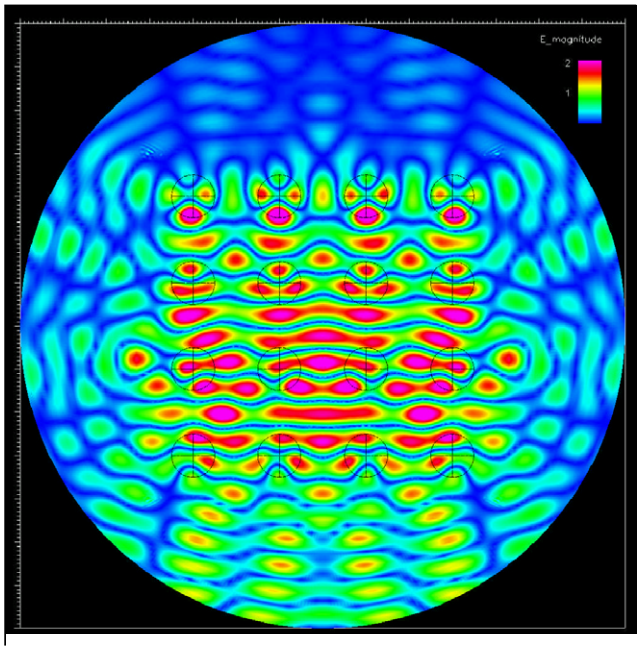

Fig 3: FDTD simulation of the scattering of a TM_z plane wave on an 4×4 cubic '2D mini crystal' of infinite dielectric cylinders with ε_r =2; λ/d =1.2, lattice parameter a=d; contour plot of $|{}_sE_z\,(r, \varphi, 2\pi\,\tau/T)|$ at random phase angle τ after steady state is reached; (solver in scattered field mode, scattered field plotted), ca. $2.5\cdot10^5$ cells

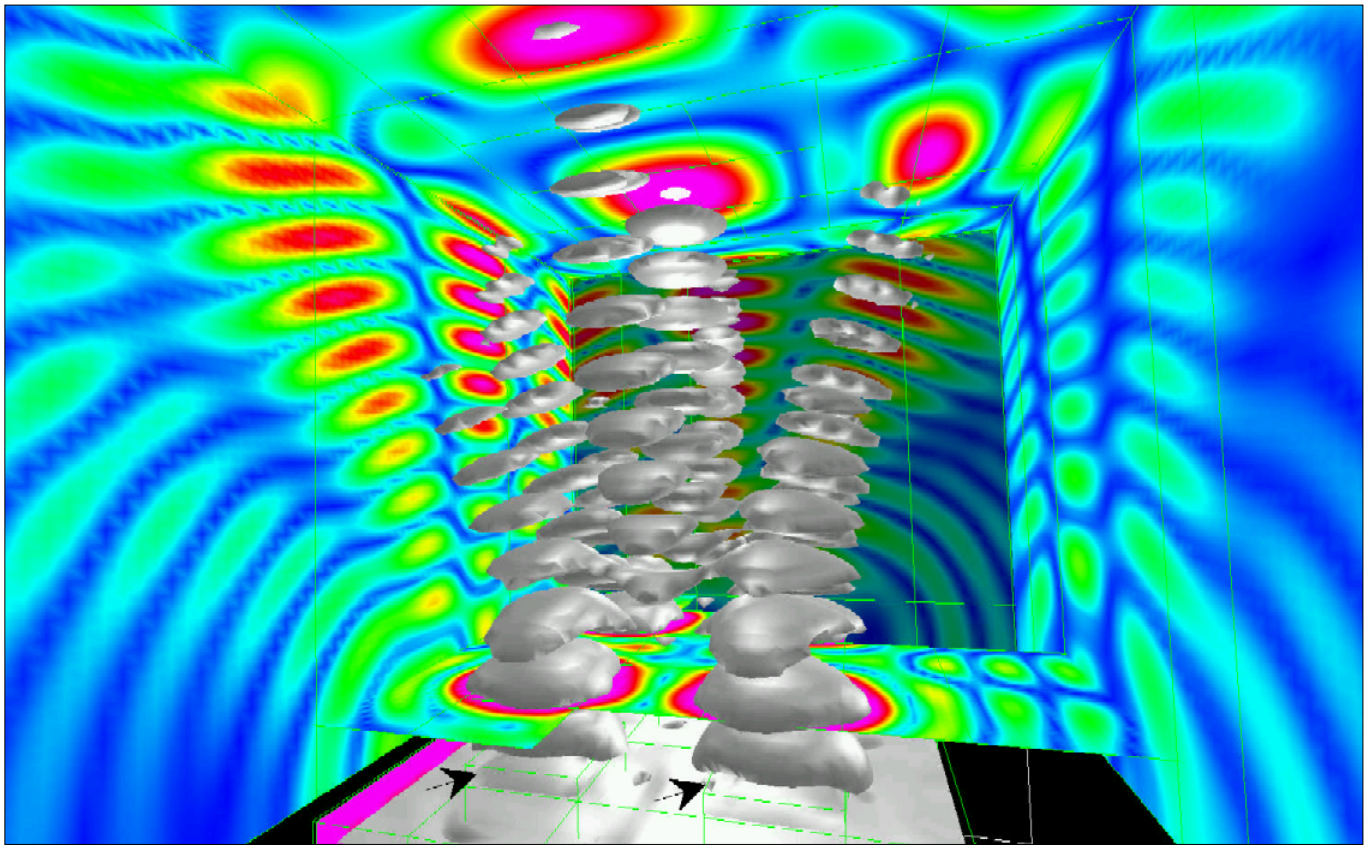

Fig 4: FDTD simulation of the scattering of a TM_x plane wave packet (propagating in +z direction coming from the bottom of the image, grey area) through a 2×2 square aperture array (each aperture's size is λ×λ, 2 apertures indicated by arrows); walls: contour plot of $|_sE(x,y,z,t)|$, volume: iso-surfaces of $|_sE(x,y,z,t)|$=0.4V/m illustrating the beam-lets exiting the apertures, notice the formation of the main diffraction maxima in the middle; plots at randomly chosen time *t*, (solver in total field mode, total field plotted), ca. 10^6 cells

REFERENCES

[1] J.B. Pendry: "Calculating Photonic Band-Structure", J. Phys. (Condensed Matter), vol. 8, 1996, pp. 1085-1108

[2] A. J. Ward and J.B. Pendry: "Refraction and geometry in Maxwell's equations", Journal of Modern Optics, 1996, Vol 43, No. 4, pp. 773-793

[3] Gadot et al.: "Photonic Band Gap Materials for Devices in the Microwave Domain", IEEE Trans. on Magnetics, vol. 34, no. 5, Sept. 1998, pp. 3028-3031

[4] Atsushi Sakai and Toshihiko Baba: "FDTD Simulation of Photonic Devices and Circuits Based on Circular and Fan-Shaped Microdisks"; IEEE Journal of Lightwave Technology, Vol. 17, No. 8, Aug. 1999

[5] Special issue of IEEE Trans. on Microwave Theory and Techniques, vol. 47, no. 11, Nov. 1999

[6] R. B. Hwang and S. T. Peng: Guided Waves on 2D Periodic Structures and Their Relation to planar Photonic Band Gap Structures"; IEICE Trans. Electron., Vol. E83-C, No. 5, May 2000, pp.705-712

[7] F.-R. Yang, R. Coccioli, Y. Qian, and T. Itoh: "Planar PBG Structures:Basic Properties and Applications"; IEICE Trans. Electron., Vol. E83-C, No. 5, May 2000, pp.687-696

[8] Tom D. Mistler: "Near-Field Optics: A New Tool for Data Storage", Proceedings of the IEEE, VOL. 88, NO. 9, Sept. 2000 pp. 1480-1490

[9] W. L. Vos, M. Megens, C. M. van Kats, and P. Bösecke: "X-ray Diffraction of Photonic Colloidal Single Crystals", Langmuir, Vol. 13, No. 23, 1997, pp. 6004-6008

[10] Constantine A. Balanis: "Advanced Engineering Electromagnetics", John Wiley & Sons, 1st edition (May 9, 1989)

[11] S.K.Sharma and D. J. Sommerferld: "On the angular location of maxima and minima in light scattered by infinite cylinders at normal incidence"; J. Phys. D., Appl. Phys. 1987, Vol. 20 (12), pp. 1661-1663

[12] Allen Taflov and Susan Hagnes: "Computational Electrodynamics: The Finite-Difference Time-Domain Method", Artech House, 2nd edition (2000)

[13] R.W. Tramel, M. Turowski, A. Przekwas, J. Schultz and R.G. Frey: "Modeling of Electromagnetic Fields in High Speed Electronic Interconnects Using a Least Squares FD-TD Algorithm", MSM2001, Hilton Head Island, South Carolina, U.S.A. March 19-21 2001